Chapter 5

Cluster Radioactivity

5.1 Prediction and Discovery of Cluster Radioactivity

The possibility to have a cluster process is related to its exotermicity:

$$Q = M(A, Z) - M(A_1, Z_1) - M(A_2, Z_2) > 0$$

Here, $M(A_i, Z_i)$ are the atomic masses. For the elements found in the second half of the periodic system, which have average binding energy per nucleon smaller than the lightest elements, this condition is fulfilled for a large range of nuclear decay. However in the great majority of cases the possibility of decay is hindered by the small barrier penetrability. This quantity reaches large values only in two cases: α-decay and spontaneous fission of heavy nuclei. An exception is given by the high penetrabilities of the daughter nuclei ^{14}C, ^{24}Ne, etc., when the complementary nucleus is close to the double magic ^{208}Pb, values which can be larger than those corresponding to the α-decay. This fact is connected to the much larger value of the ratio Q_C/B_C relative to the value Q_α/B_α, where $B_{C,\alpha}$ are the heights of the corresponding barriers.

The investigation of this new type of radioactivity revealed some universal properties:

1. The kinetic energy of the emitted fragment, at the extent of the precision allowed by the dectors, is close to the its kinematical threshold, i.e. the residual nucleus is found in the ground state, or in a low-lying excited state, with an excitation energy $E^* \leq$1.5 MeV. Fine structure in cluster decay was observed in the case of the decay ^{223}Ra $\rightarrow$ ^{209}Pb+^{14}C when the the excited state 11/2$^+$ of ^{209}Pb is populated in proportion of 84$\%$.

2. With some exceptions all the mother nuclei are found in the actinide region, whereas the daughter nuclei, produced by the cluster emission are lying in the rather small region of charge and mass 80$\leq Z \leq$83, 206$\leq A \leq$212. These nuclei are splitting in neighbouring nuclei with a large binding energy per nucleon B/A as a consequence of the vicinity of the double magic ^{208}Pb. The large binding energy is naturaly related to the large Q-value of the decay which consequently is increasing the bariers penetrability.

3. The comparison of the spontaneous fission half-live and the cluster radioactivity half-lives revealed that the ratio $T_{1/2}^{s.f.}/T_{1/2}^{c}$ does not stay constant but increase sharply with the charge of the mother nucleus.

The Gamow-like decay rate for the CR must be changed in order to take into account the preformation factor:

$$\lambda_C = \nu P_0 S \tag{5.1}$$

The three quantities entering in the above formula are:

- The assault frequency ν which is generally associated with the zero point vibration energy E_v

  $$\nu_0 = \frac{2E_v}{h} \tag{5.2}$$

  with E_v obtained either empirically or in the harmonic oscillator approximation inside the potential pocket($E_v = \hbar\omega_0/2, \omega = \sqrt{C/M}$, with M the mass of the parent nucleus and C, the stiffness of the oscillator).

  In the preformed cluster model [1] it is considered that at the left of the first turning point ($R \leq R_i$) the kinetic energy $\mu v^2/2$ equals approximately the potential depth. A realistic potential depth is of the order $A_1 \cdot 25$ MeV corresponding to a 100 MeV deep α-nucleus potential. Then, the assault frequency is given as

  $$\nu = \frac{1}{R_i}\sqrt{\frac{25A}{2A_1}} \tag{5.3}$$

  which is nearly constant for all decay modes because the reduced mass μ scales roughly with a.

- The barrier penetrability P_0 which in the WKB approximation is given by formula (2.198), with $E_0 \equiv Q$.

- S is the bulk spectroscopic factor. This quantity is defined on the basis of the many-body states of the parent and daughter nucleus, and of the emitted cluster, which are denoted by $\phi_{A_1+A_2}$, ϕ_{A_2}, ϕ_{A_1}. The open channel state describes the relative motion of the clusters ϕ_{A_1} and ϕ_{A_2} as a superposition of the basis states

  $$\langle \boldsymbol{r}_1, \ldots, \boldsymbol{r}_{A_1+A_2-1} \mid \boldsymbol{R}\rangle = \mathcal{A}(\delta(\boldsymbol{R} - \boldsymbol{r}_{A_1A_2})\phi_{A_1}\phi_{A_2}) \tag{5.4}$$

  with different values of $\boldsymbol{R}$. In coordinate space the states $|\boldsymbol{R}\rangle$ depend on $(A_1 + A_2 - 1)$ coordinates which are equivalent to the $(A-1)$ internal coordinates of the daughter nucleus ϕ_{A_2}, the $A_2 - 1$ internal coordinates of the emitted fragments and the relative motion coordinate $\boldsymbol{r}_{A_1A_2}$. Due to the antsymmetrization $\mathcal{A}$ the states $|\boldsymbol{R}\rangle$ are not normalized

  $$\langle \boldsymbol{R} \mid \boldsymbol{R}'\rangle = (1 - \hat{K})_{\boldsymbol{R},\boldsymbol{R}'} = \delta(\boldsymbol{R} - \boldsymbol{R}') - K(\boldsymbol{R}, \boldsymbol{R}') \tag{5.5}$$

  The projection operator $\hat{P}$ onto the open channel space $\{|\boldsymbol{R}\rangle\}$ is defined as

  $$\hat{P} = \int d^3R \int d^3R' \boldsymbol{R} \left(\frac{1}{1-\hat{K}}\right)_{\boldsymbol{R},\boldsymbol{R}'} \langle \boldsymbol{R}' \mid \tag{5.6}$$

The inverse of the norm operator $1 - \hat{K}$ guarantees that $\hat{P}^2 = \hat{P}$. Then, the spectroscopic factor equals the percentage to which the state $\phi_{A_1+A_2}$ lies in the space $\phi_{A_1} \otimes \phi_{A_2}$:

$$S = \langle \phi_{A_1+A_2} \mid \hat{P} \mid \phi_{A_1+A_2} \rangle \tag{5.7}$$

In other words, S is the quantum mechanical probability of finding the open channel structure preformed in the parent nucleus, and for that reason it also called preformation probability and can be related to the squared product of the overlaps between the single particle states in ϕ_{A_1} and the upper ones in $\phi_{A_1+A_2}$ forming the fragment. The product contains effectively $A_1 - 1$ single particle overlaps because ϕ_{A_1} depends on $A_1 - 1$ internal coordinates. This structure implies that many single particle states contribute to S, and that S will approximately scale with the $(A_2 - 1)$-st power of the square of a single-particle overlap. The first point suggests to use the bulk formula

$$S = (S^\alpha)^{\frac{A_1-1}{3}}, \qquad (A_1 \leq 28) \tag{5.8}$$

where the α spectroscopic factor S^α is fitted to the empirically estimated preformation S^{emp}. Fittting the even and odd parents separately, Blendowske and Walliser obtained in the case of favored decays [2]:

$$(S^\alpha)^{\text{even}} = 6.3 \times 10^{-3} \quad \text{and} (S^\alpha)^{\text{odd}} = 3.2 \times 10^{-3} \tag{5.9}$$

For rapid evaluations of the decay constant there is available a simple analytical formula which is used for α-decay and all cluster decays. Instead of a realistic heavy-ion potential a square well with suitable radius R_i is used. The nearly A_1-independent assault frequency $\nu = v/2R_i$ is fixed to an appropriate numerical value. The resulting decay constant is then given by

$$\lambda_C \approx \nu S_\alpha^{\frac{A_1-1}{3}} \exp(-2I), \qquad \nu = 3.0 \cdot 10^{21} \text{s}^{-1}, \qquad S_\alpha = 6.3 \times 10^{-3} \tag{5.10}$$

the penetration integral for the pure Coulomb potential can be evaluated analitically [3]:

$$I = Z_1 Z_2 e^2 \sqrt{\frac{2\mu}{\hbar^2 (Q - E^*)}} \left\{ \text{acos}(\sqrt{x}) - \sqrt{x(1-x)} \right\} \tag{5.11}$$

with

$$x = \frac{R_i (Q - E^*)}{Z_1 Z_2 e^2}, \qquad R_i = 1.286 \left(A_1^{1/3} + A_2^{1/3} \right) \tag{5.12}$$

In addition one uses $\hbar^2/(2\mu)$=20.9$(A_1 + A_2)/(A_1 A_2)$ Mev·fm^2 and e^2=1.443 MeV·fm. Up to A_1=34 all decay constants are reproduced within a factor of 3.

5.2 Cold Valleys as Doorways of Cluster Radioactivity

The concept of *Cold Valley* was introduced in relation to the structure of minimas in the so-callled driving potential. The driving potential is defined as the difference between the interaction potential and the decay energy of the reaction

$$V_{\text{driv}} = V(R, Z_1, A_1, \{\beta^{(1)}\}_{2,3,4}, \{\beta^{(2)}\}_{2,3,4}, \omega_1, \omega_2) + B_1 + B_2 - B_{\text{CN}} \tag{5.13}$$

In the above formula B_1, B_2 and B_{CN} are the binding energies of the cluster, daughter and mother nucleus. The driving potential is also depending on the charge Z_1, mass A_1, the distance between the centres-of-masses of the two nuclei R, mutual orientations $\omega_{1,2}$ and the quadrupole(β_2), octupole (β_3) and hexadecupole deformations (β_4) through the heavy ion potential V defined in (3.68). The above *Ansatz* corresponds to the s-channel, i.e. relative angular momentum $l = 0$.

A long time ago Săndulescu *et al* investigated the occurence of fusion valleys as doorways to the synthesis of superheavy elements [4, 5]. The basic idea of this approach was to calculate the driving potential of a given compound nucleus for all possible projectile-target combinations as $\eta_Z = (Z_1 - Z_2)/(Z_1 + Z_2)$ at the touching point R_c, i.e. the point where the assumed spherical fragments are coming in contact and they interact only by means of the Coulomb force. The charges of the target and the projectile were determined by requiring for a fixed η that the potential $V(R, \eta, \eta_Z)$ attains a minimum in the η_Z direction, i.e. for every fixed mass pair (A_1, A_2) a single pair of charges is determined among all possible combinations. Next, minimas of the potential in the two-dimensional (R, η) landscape were searched. From here it was inferred a criterion for cold fusion, i.e. the deep minima of the driving potential are corresponding to the projectile-target combinations where the compound nucleus has a minimum of excitation and will de-excite to the ground-state with the emission of a couple of neutrons. The occurence of the mass-asymmetry valleys is due to the shell effects. It was advocated in ref. [6], using the frame of the fragmentation theory, that due to the existence of different mass-asymmetry valleys for the same compound system, a new, highly asymmetric fission mode appears in which one of the fragments is close to the double magic nucleus ^{208}Pb. This new type of decay is nothing else than the cluster radioactivity.

Formation of cold fusion valleys is strongly dependent on which shape is assumed for the incoming projectile and target. For the case when one assumes spherical shapes, as actually was done in [4, 5] and more recently in [7], the most important valleys found are centered around the double magic nuclei ^{132}Sn (a weak asymmetric valley) and ^{208}Pb (a very asymmetric valley). The introduction of deformation modifies the valley structure of the driving potential [8]. The valleys occuring when nuclei are assumed to be spherical are weakened or even washed out when the experimental or calculated ground state deformations of the nuclei are switched on. Instead, other valleys are substantiated, depending crucially on the mutual orientation of the nuclei as it was proved recently [8].

5.2.1 Cluster Radioactivity in ^{114}Ba

As we mentioned in the Introduction, the neutron deficient nucleus ^{114}Ba was predicted to decay in the ^{12}C and the almost double magic ^{102}Sn. The inspection of the corresponding driving potential in Fig.5.1 confirms this prediction. Along with the ^{12}C minimun there are two other comparable minima, one to its left, ^{8}Be, and the second to its right, ^{16}O. The prevailance of the ^{12}C-channel compared to the other two is given by the magicity of the partner ^{102}Sn.

It is interesting to notice that all minima are corresponding to $N = Z$ clusters, and that from the most asymmetric minimum, α+^{110}Xe up to to the splitting ^{28}Si+^{86}Mo these minima are separated by rather higher barriers and can be joined by a continous chain of α-particles, the splitting ^{12}C+ ^{102}Sn being a relative minimum on this curve. This would

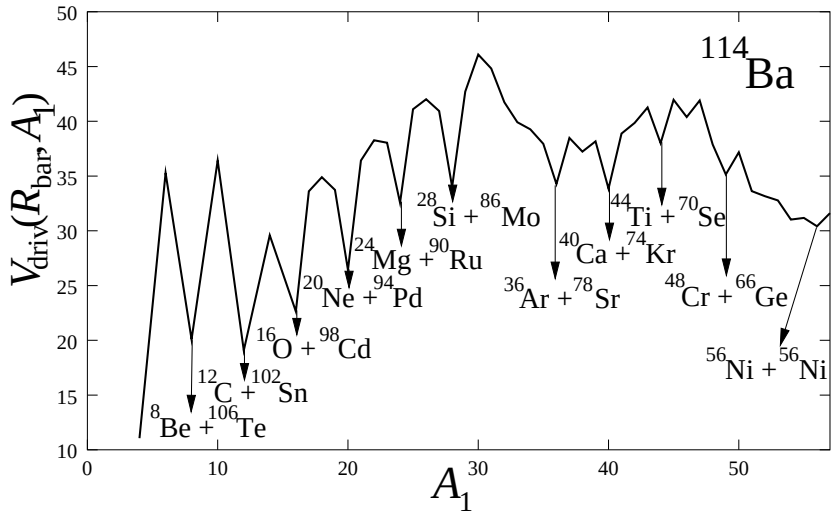

Figure 5.1: The driving potential of ^{114}Ba.

mean that if we imagine the reverse process and we collide ^{28}Si with ^{86}Mo it is energetically more favorable to transfer α-particles in order to reach the compound nucleus than to initiate single-nucleon, di-neutron or di-proton transfer. Eventually the dinuclear system will land on the "α-like valley" ^{12}C+ ^{102}Sn and a part of the flux will be lost by quasi-fission and the rest of the flux will move further in the direction of the compound nucleus by crossing the "α-like barrier" ^{8}Be+ ^{106}Te.

5.2.2 Cluster Radioactivity in Radium and actinides

The cold valleys in the case of CR are strongly dependent on the deformation of the clusters and daughter nuclei. In the case of ^{222}Ra the most pronounced valley corresponds to the case ^{14}C+^{208}Pb, both nuclei being spherical (see Fig.5.2). However beyond the cluster mass number $A_1 = 16$ the deformation cause the deviation of the $e - e$ curve from the $p - p$ one. The existence of the valley corresponding to the emission of the cluster ^{14}C and the double-magic daughter nucleus ^{208}Pb is confirmed in experiment [9]. Simmilarly happens to the Radium isotopes 221, 223, 224 and 226.

At the other extreme of studieded cluster emitters, i.e. ^{242}Cm, we are inferring from Fig.5.3 that the cluster valleys are shifted to larger cluster masses. In the case of $p - p$ configuration the deepest valley corresponds to the splitting ^{40}S+^{202}Hg and the second important valley is the recently reported splitting ^{34}Si+^{208}Pb [10]. This last valley is less favourable in the frame of the cold valley picture of decay because of the sphericity of both cluster, ^{34}S, and daughter nucleus ^{208}Pb which rises sensitively the barrier compared to the case of the prolate (β_2 =0.254) cluster, ^{40}S, emitted at the equator of the oblate(β_2 $\approx$-0.09) mother nucleus ^{202}Hg. As one can see from Fig.5.3 if the cluster ^{40}Si would be emitted at the pole of ^{202}Hg, with its symmetry axis perpendicular to the axis joining the centers of the two nuclei($e - e$ configuration), then the corresponding valley would lose completely in importance and the only observed cluster decay should be ^{34}Si+^{208}Pb. Of course that the spectroscopic factors may invert the importance of these two valleys by favouring the clusterization of the double

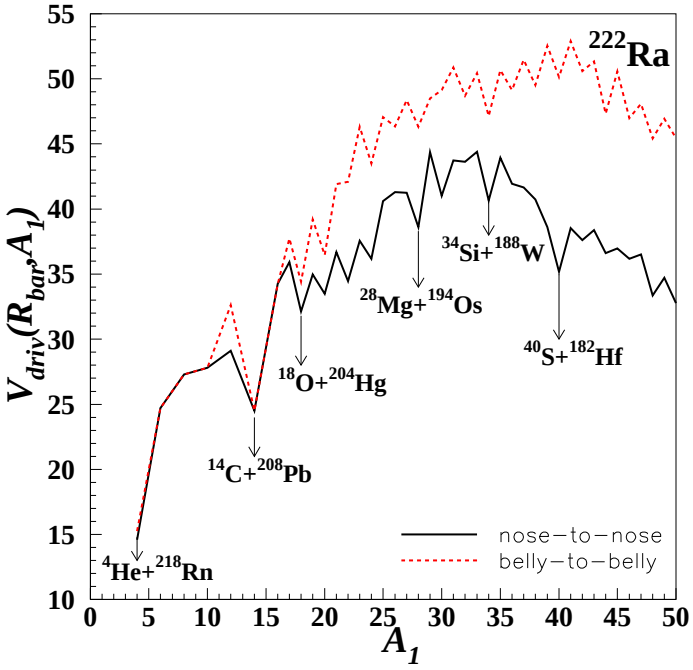

Figure 5.2: Comparison between the $p-p$ and the $e-e$ oriented driving potentials for the mother nucleus ^{222}Ra.

magic ^{208}Pb. It is therefore necessary that the investigation of the cluster emission in ^{242}Cm looks for both splittings and not only of ^{34}Si+^{208}Pb.

Thorium

In the case of Th, where cluster radioactivity has been observed, we draw in Fig.5.4 the driving potential in $p-p$ configuration for four of its even-even isotopes. For all 4 investigated isotopes we indicated the corresponding α-decay which is the predominant cluster emission mode. For ^{226}Th the first two deepest cluster valleys are given by the combinations ^{14}C+^{212}Po and ^{18}O+^{208}Pb, and are actually experimentally confirmed cluster emission channels. We notice here that ^{226}Th is the only isotope of Th where one observes the emission of ^{14}C. For ^{228}Th the deepest minimum is encountered for the splitting ^{20}O+^{208}Pb which is the only observed cluster emission channel up to now [11]. The splittings, ^{14}C+^{214}Po and ^{22}Ne+^{206}Hg, although not observed, are also corresponding to deep valeys, and we put a question mark(?) to stress that their possible observation in the future should not be excluded. Moving two neutrons further at ^{230}Th we find that the deepest minimum moved two cluster charge numbers further and corresponds to the observed splitting ^{24}Ne+^{206}Hg [12]. However the neighbouring splittings ^{20}O+^{210}Pb and ^{22}O+^{208}Pb have also close values of the minima but they were not recorded in experiment. Also the ^{14}C emission channel should be favorable for ^{230}Th according to the cold valley approach but no experimental evidence was provided to the date. The last Thorium's isotope, ^{232}Th, is the most rich in compa-

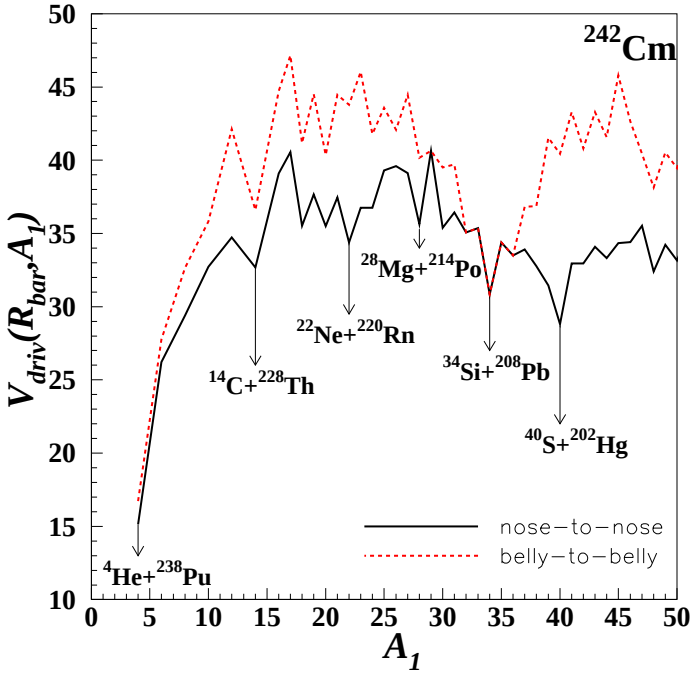

Figure 5.3: Same as in Fig.5.2 for ^{242}Cm.

rable deep valleys. If we leave aside the valley of ^{14}C+^{218}Po, then the deepest one is the experimentally confirmed splitting ^{24}Ne+^{208}Hg. Also observed is the neighbouring splitting ^{26}Ne+^{206}Hg. The other minimas corresponding to the emission of ^{20,22}O and ^{28,30}Mg are not yet experimentally registred.

One may conclude that the reason of the decrease in importance of ^{14}C emission when moving from ^{226}Th to ^{232}Th is due to the corresponding daughter nucleus, i.e. Polonium. By adding more and more neutrons to Po, we get away from the neutron magic shell and most likely the spectroscopic factors are decreasing. The probability of reaching different cold valleys from the ground state (cluster preformation) should come into play.

If one cheks the deformations of the emitted clusters one finds that that the deepest valleys for ^{228,230,232}Th are corresponding to high quadrupole and/or hexadecupole distortions which indicate a possible subcluster strucure, as is the case of ^{20}O+^{208}Pb, ^{24}Ne+^{206}Hg and ^{24}Ne+^{208}Hg.

It is also worthwile to notice for the case of Thorium that the cluster radioactivity cold valleys are grouped in "super-valleys" which are broader when moving to larger neutron numer of the mother nucles. For the emitter ^{228}Th we have a "super-valley" which ranges from cluster mass A_1=18 to 24 whereas for ^{232}Th it ranges A_1=18 to 30.

Uranium

For Uranium we take as well 4 even-even isotopes which are known cluster emitters(see Fig.5.5). The mother nucleus ^{230}U has a very pronounced valley centered on the splitting

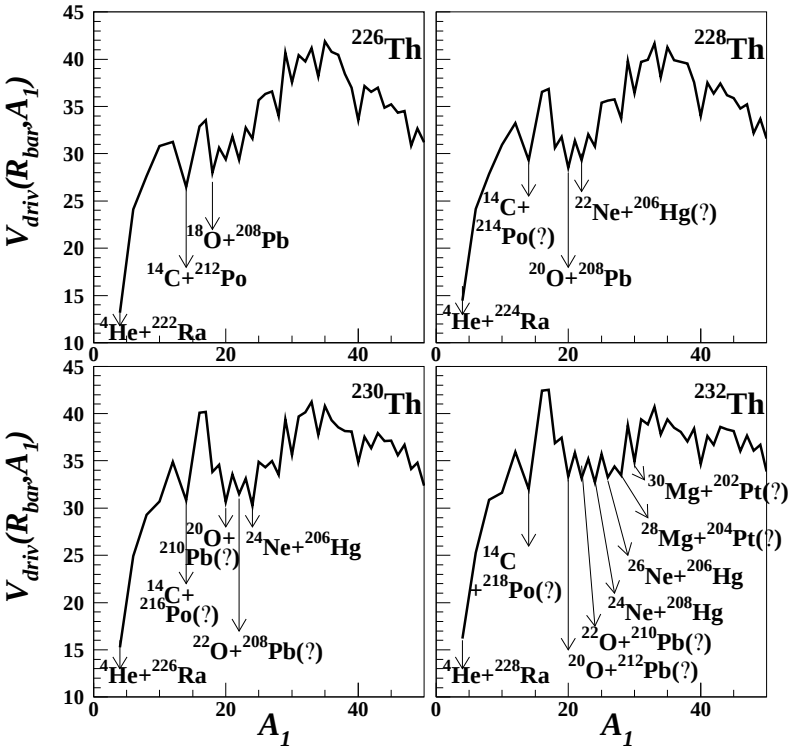

Figure 5.4: The driving potential of ^{226,228,230,232}Th in the $p-p$ configuration. The question mark (?) indicates that the given combination, although not observed in experiment, has a favorable position in the cold valley.

^{22}Ne+^{208}Pb, which is actually the only case of observed CR for this nucleus. The reason for obtaining such a deep minimum is due not only to the double magicity of the daughter nucleus, but also to the large cluster's quadrupole (β_2=0.326) and especially hexadecupole (β_4=0.225) deformations. For the next isotope, ^{232}U, the minimum shifts on the cluster ^{24}Ne, which is oblate(β_2 =-0.215), and in order to overcome a smaller barrier, it should be emitted with its simmetry axis perpendicular to the fission axis. Adding two more neutrons, we obtain two comparable minimas for ^{24}Ne+^{210}Pb and ^{28}Mg+^{206}Hg. In between we have the combination ^{26}Ne+^{208}Pb which although is not giving a minimum in the driving potential is shares the same valley as ^{28}Mg+^{206}Hg. It is important to stress that the clusters of all these three splittings, which were also reported by experiment [13], have large quadrupole deformations and especially hexadecupole deformations. The last investigated isotope of Uranium, ^{236}U has less pronounced minimas, but like in the previous cases, two cluster decay channels were observed in experiment, corresponding to two deep minima, ^{28}Mg+^{208}Hg and ^{30}Mg+^{206}Hg. In the first case we deal with a prolate cluster and in the second with an oblate cluster, both endowed also with a sensitive negative hexadecupole deformation.

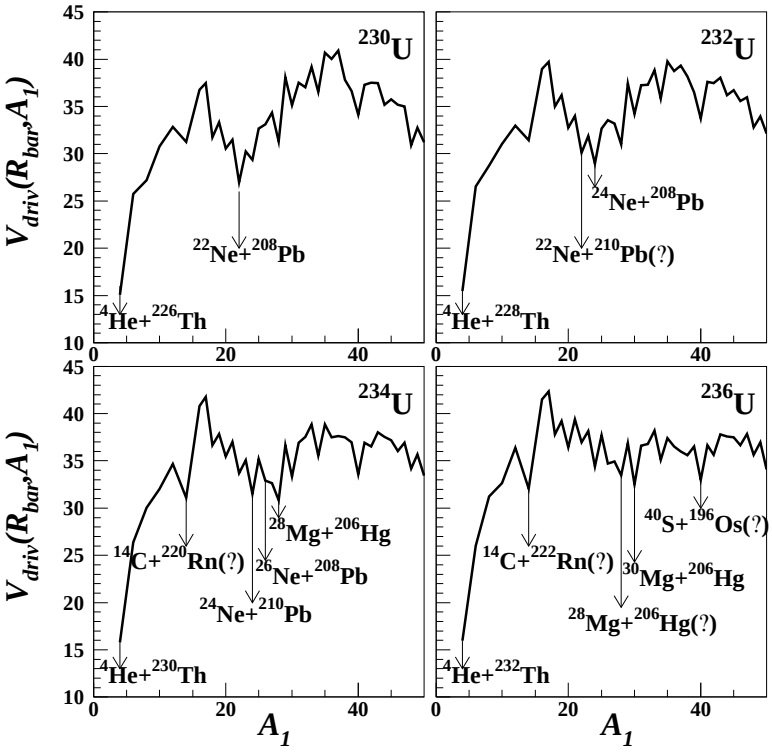

Figure 5.5: Same as in Fig.5.4 for ^{230,232,234,236}U.

Actually for the two isotopes ^{234,236}U we obtained that the deepest minima corresponds to ^{14}C because it enters in combination with Rn isotopes which are increasingly deformed. However the emission of ^{14}C was not observed in any isotope of Uranium which means that we deal with a hindrance in the preformation of such combinations, the main responsible, in our opinion, being the daughter nucleus which preferes to acquire a spherical or almost spherical shape, in the neighbourhood of the double-magic ^{208}Pb. Everything is going on as if the heavier(daughter) nucleus, is transferring nucleons, or even clusters, untill it reaches the valley containing spherical or almost spherical isotopes of Pb and Hg. In the same time the cluster is acquiring quadrupole and hexadecupole deformation mainly, having in almost cases a clear clusterized structure which indicates that it is possible that a sequencial transfer of alphas is taking place. For the case of the cluster ^{22}Ne we can enview for example the transfer of two alphas to the spherical ^{14}C which are leading to a large hexadecupole deformations with the two alphas arranged at the opposite ends of ^{14}C.

For the investigated isotopes of Uranium we should also remark, when increasing the number of neutrons, the gradual weakening of the cluster valley and the increase in importance of the minimum corresponding to the splitting ^{40}S+$^{A-40}$Os. However, we expect in this case like for ^{14}C a hindrance in the preformation.

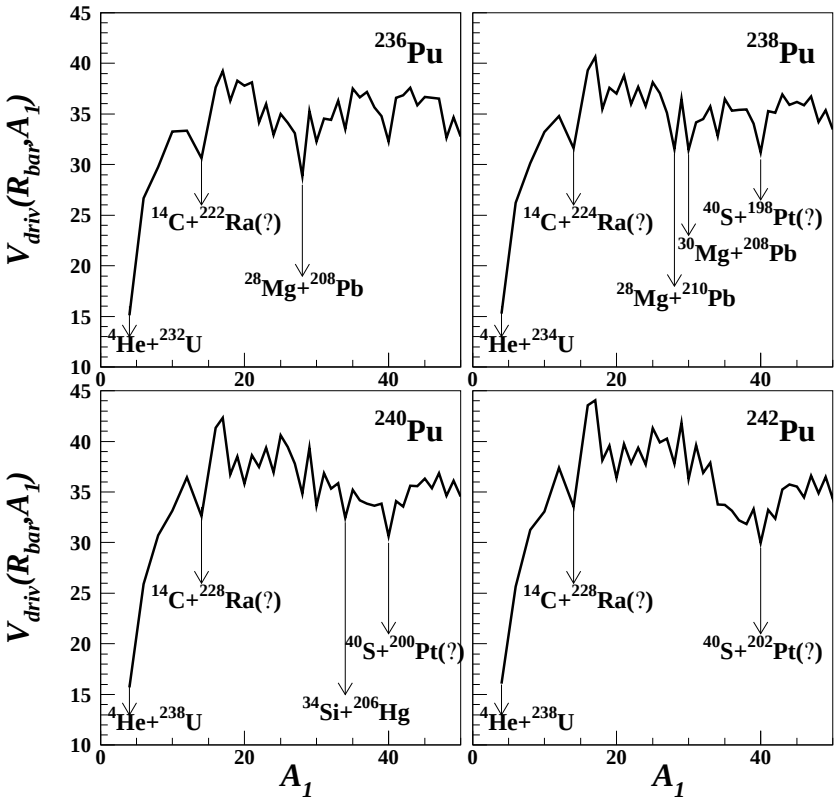

Figure 5.6: Same as in Fig.5.4 for ^{236,238,242,244}Pu.

Plutonium

In the case of Plutionium (Fig.5.6) we remark for its lowest mass number isotope, ^{236}Pu, were CR is observed, that a very deep minima is obtained for the splitting ^{28}Mg+^{208}Pb. This is also the only case of emitted heavy cluster confirmed by experiment. For ^{238}Pu the experimentally observed splittings ^{28}Mg+^{210}Pb ^{30}Mg+^{208}Pb and ^{32}Si+^{206}Hg are competed in the driving potential by the splitting ^{40}S+^{198}Pt. However, it is expected that this last splitting should have a smaller spectroscopic factor compared to the first two splittings, due to the lack of magicity in the proton and neutron numbers of the cluster and daughter nucleus. The next even isotope, ^{240}Pu exhibits a deep minimum on the observed decay mode ^{34}Si+^{206}Hg. However the minimum on ^{40}S+^{200}Pt is deeper.

To the date, no cluster emission was observed for ^{244}Pu. However a pronounced minimum is obtained in the present calculations for the cluster ^{40}S. For ^{244}Pu we notice the occurence of two close minima, ^{38}Si+^{206}Hg and ^{40}S+^{204}Pt in which both daughter nuclei posses a magic neutron number (N=126).

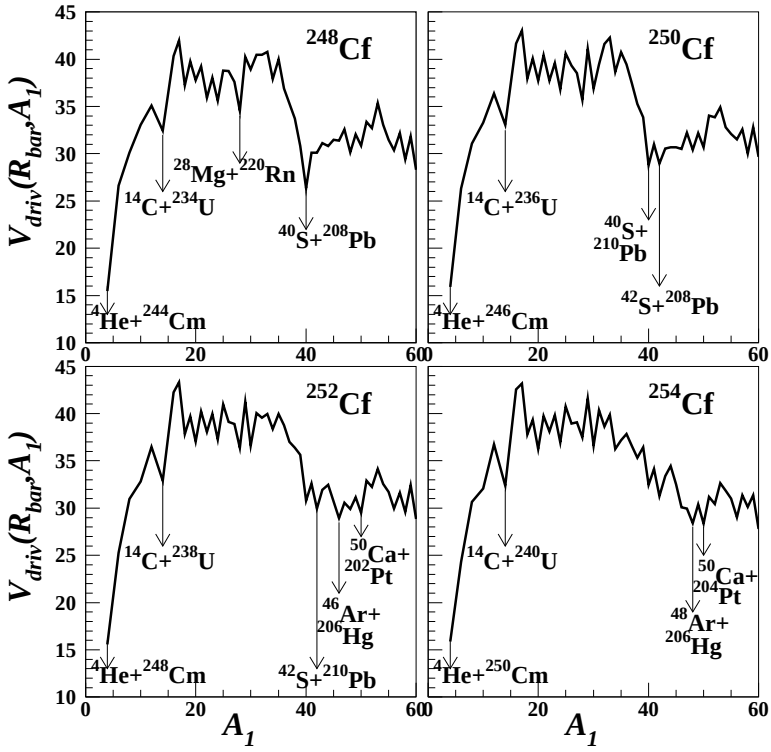

Figure 5.7: Same as in Fig.5.4 for ^{248,250,252,254}Cf.

Californium

Results for Californium isotopes are displayed in Fig.5.7. The first isotope of Californium that we considered is ^{248}Cf. By far the most deep minimum corresponds to the splitting ^{40}S+^{208}Pb. The cluster is predicted by the macroscopic-microscopic model [14] to be prolate deformed (β_2=0.254) which lowers sensitively the barrier. Together with that comes the double magicity of ^{208}Pb. For ^{250}Cf, there are two shallower minima in competition in the same region, i.e. ^{40}S+^{210}Pb and ^{42}S+^{208}Pb. Adding two more neutrons causes the broadening and shifting further to the right of the valley. Minima for the spherical clusters ^{46}Ar, ^{48}Ca and ^{50}Ca are occuring this time due to the magic neutron shell, N=126, of the corresponding daughter nuclei, ^{206}Hg and ^{204}Pt. A third minimum comes from the splitting ^{42}S+^{210}Pb. The last investigated isotope of Californium, ^{254}Cf, has the same feature as the previous one, i.e. predominance of the neutron magic number.

We notice also in the case of Californium the weakening and spreading of what we believe to be CR valley when one increases the number of neutrons.

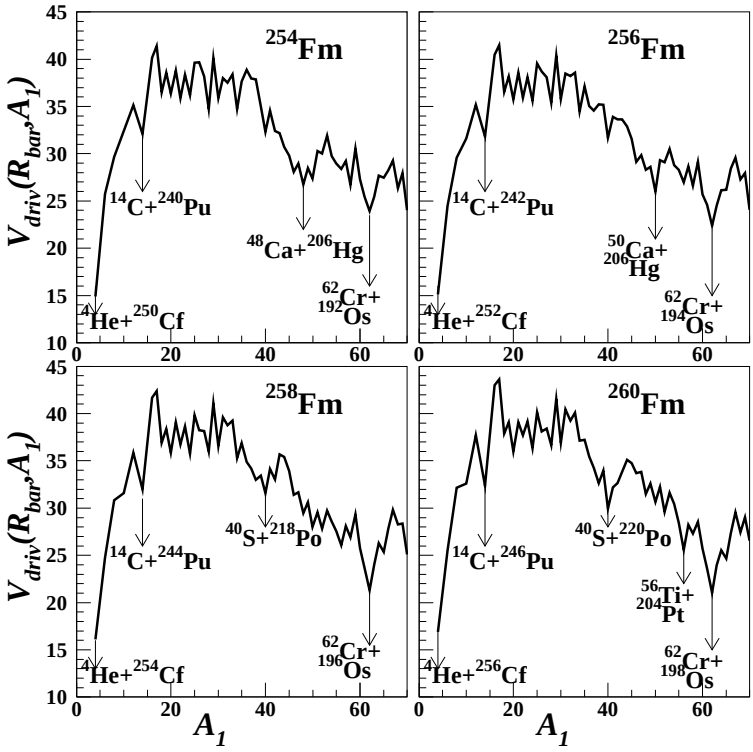

Figure 5.8: Same as in Fig.5.4 for ^{254,256,258,260}Fm.

Fermium

For Fermium we investigated the isotopes with mass numbers A=254-260. and extended the range of cluster mass numbers up to $A_1 = 70$. The $Fe - Cr$-valley, important also for superheavy elements [8], is very stable for all four isotopes and centered on ^{62}Cr(see Fig.5.8). Obviously in this case the cluster mechanism remarked for the known cluster emitters is apparently not essential, both partners of the splitting having no magic proton or neutron numbers. This is a typical example of a valley where the dictating criteria is the quadrupole and hexadecupole deformation[8]. Besides that we expect small preformation factors compared to lighter clusters, due to the increasing mass and lack of magicity. In what concerns valleys of lighter clusters we easily identify for ^{254,256}Fm, a Calcium valley, where the magicity is a property of both cluster and daughter nuclei. For ^{258,260}Fm this valley is washed out and the minimum corresponding to ^{40}S gains in importance.

Bibliography

[1] R.Blendowske, T.Fliessbach and H.Walliser, Nucl.Phys.**A464**, 75 (1987).

[2] R.Blendowske and H.Walliser, Phys.Rev.Lett.**61**, 1930 (1988).

[3] D.N.Poenaru, M.Ivascu, A.Sandulescu and W.Greiner, preprint E4-84-446 JINR-Dubna (1984).

[4] A.Săndulescu, R.K.Gupta, W.Scheid and W.Greiner, Phys.Lett.**60B**, no.3 (1976) 225.

[5] R.K.Gupta, A.Săndulescu and W.Greiner, Phys.Lett.**67B**, no.3 (1976) 257.

[6] A.Săndulescu and W.Greiner, J.Phys.G**3** (1977) L189.

[7] R.A.Gherghescu, D.N.Poenaru and W.Greiner, J.Phys.G**23** (1997) 1715.

[8] Ş. Mişicu and W.Greiner, Phys.Rev.C **65**, 044606 (2002)

[9] P.B.Price, J.D.Stevenson, S.W.Barwick and H.L.Ravn, Phys.Rev.Lett.**54**, 297 (1985)

[10] A.A. Oglobin et al., Phys.Rev.**C61**, 034301 (2000). R.Bonetti, V.A. Denisov, A.Gugliemetti, M.G.Itkis, C. Mazzochi, V.L.Mickheev, Yu.Ts. Oganessian, G.A. Pik-Pichak, G.Poli, S.M. Pirozhkov, V.M.Semockhin, V.A.Shigin, I.K.Shvetsov and S.P.Tretyakova,

[11] R.Bonetti et al., *Contr. 6th Int. Conf. on Nucl. Reaction Mechanisms*, Varenna, June 101-5, 1991, p.333.

[12] S.P.Tretyakova, A.Sandulescu, V.L. Micheev, D.Hasegan, I.A. Lebedev, Yu.S.Zamyatnin, Yu.S.Korotkin and B.F. Myasoedov, Rapid Comm. JINR Dubna (1985).

[13] S.Wang, P.B.Price, S.W.Barwick, K.J.Moody and E.K. Hulet, Phys.Rev.**C36**, 2717 (1987).

[14] P. Möller, J.R. Nix, W.D. Myers and W.J. Swiatecki, At.Data Nucl. Data Tables **59**, 185 (1995).